Electromagnetic waves on ion gyro-radii scales across the magnetopause

Y. Yao,[1] C. C. Chaston,[1] K.-H. Glassmeier,[2] and V. Angelopoulos[3]

Received 1 March 2011; revised 4 April 2011; accepted 4 April 2011; published 14 May 2011.

[1] This report presents the first study of the global distribution and properties of kinetic scale electromagnetic waves on the Earth's magnetopause. From a statistical study using THEMIS fields observations over a frequency range from 0.01–2 *Hz*, we find waves on scales of the order of ion gyro-radii at all magnetic local times surveyed (4–20 MLT). The spectral energy densities (ϵ) within these waves across the magnetopause are larger on the dawn (4–12 MLT) than duskside (12–20 MLT) irrespective of the direction of the magnetosheath magnetic field B_{Z_sheath} component. Furthermore, these observations reveal that ϵ is magnetic shear dependent with large enhancements for shear angle >60°. The similarity between dawn-dusk asymmetry in ϵ we observe and reported distribution of magnetosheath ions in the magnetosphere suggest that gyro-radii scale magnetic field structures/waves may facilitate a significant fraction of cross magnetopause plasma transport. **Citation:** Yao, Y., C. C. Chaston, K.-H. Glassmeier, and V. Angelopoulos (2011), Electromagnetic waves on ion gyro-radii scales across the magnetopause, *Geophys. Res. Lett.*, *38*, L09102, doi:10.1029/2011GL047328.

1. Introduction

[2] The Earth's magnetopause is a transition layer between the shocked plasmas of interplanetary space and those of the magnetosphere. It is a critical region for solar wind-magnetosphere coupling because the structure and dynamics of the magnetopause alter the rate of mass, momentum and energy transport from the solar wind into the magnetosphere [*Paschmann*, 1997]. These rates are determined by physical interactions, which occur on small scales where the frozen-in approximation is violated and relative motion between the plasma and magnetic fields can occur. The largest of these scales include the ion inertial length at which scale magnetic reconnection can occur [*Mozer et al.*, 2002], and the ion gyro-radius (ρ_i) at which scale regular cyclotron motion can be disrupted and electric fields parallel to the magnetic field facilitate cross-field transport and heating [*Hasegawa and Mima*, 1978]. Electromagnetic features on ion gyro-radii scales are often described as kinetic Alfvén waves (KAWs) [*Hasegawa and Chen*, 1975], and their role in particle heating/acceleration and plasma transport across the magnetopause has been considered by several authors [*Hasegawa and Mima*, 1978; *Rezeau et al.*, 1989; *Lee et al.*, 1994; *Johnson and Cheng*, 1997, 2001; *Chaston et al.*, 2007].

[3] While direct observations of plasma transport across the magnetopause are experimentally challenging [*Paschmann*, 1997], its consequences are well established and reveal distinct features that can be checked against proposed entry mechanisms. For example, observations from the Geotail and DMSP spacecrafts have revealed a dawn-dusk asymmetry during periods of northward interplanetary magnetic field (IMF) in the distribution of cold magnetosheath ions in the boundary layer and plasma sheet [*Hasegawa et al.*, 2003; *Wing et al.*, 2005] and certain MLT 'hot spots' [*Nishino et al.*, 2007]. The MLT dependence of magnetosheath ion observations in the dayside magnetosphere implies that there is an MLT dependence in the entry mechanisms. To determine if such a distribution can be expected from KAW driven transport we have performed a statistical study using THEMIS fields observations to analyze the MLT distribution of the spectral energy density of gyro-radii scale magnetic field structures. From a dispersion analysis these structures are shown to have the properties of KAWs. To determine how this distribution varies with the orientation of the magnetic field through the magnetosheath these results are categorized according to the orientation of B_{Z_sheath} (GSE) component in the magnetosheath and magnetic shear angle (θ_B) observed across the magnetopause.

2. Observations

[4] Figure 1 presents a case study of a magnetopause crossing (MPC) observed from probe B of the THEMIS mission [*Sibeck and Angelopoulos*, 2008]. As indicated by the labeling at the top of Figure 1, the spacecraft travels from the magnetosphere through a boundary layer and across the magnetopause into the magnetosheath. These transitions can be identified through the distinct jumps in density and temperature shown in Figure 1a and the steps in the ion energy spectra shown in Figure 1b as measured by the Electrostatic Analyzer (ESA) instrument [*McFadden et al.*, 2008]. The boundary layer is composed of a mixture of hot magnetospheric plasmas and the warm plasmas of the magnetosheath. We note that in this case the magnetopause population has been accelerated to energies intermediate between that of the magnetosphere and the magnetosheath. The magnetopause traversal is identified by the rotation of the magnetic field shown in Figure 1d as measured by the Fluxgate Magnetometer (FGM) instrument [*Auster et al.*, 2008]. Significantly in this case the B_Z (GSE) component undergoes a reversal from positive to negative on field-lines dominated by magnetosheath plasmas. This field reversal together with the accelerated magnetosheath

[1]Space Sciences Laboratory, University of California, Berkeley, California, USA.
[2]Institut für Geophysik und Extraterrestrische Physik, Technische Universität Braunschweig, Braunschweig, Germany.
[3]Institute for Geophysical and Planetary Physics, University of California, Los Angeles, California, USA.

0094-8276/11/2011GL047328

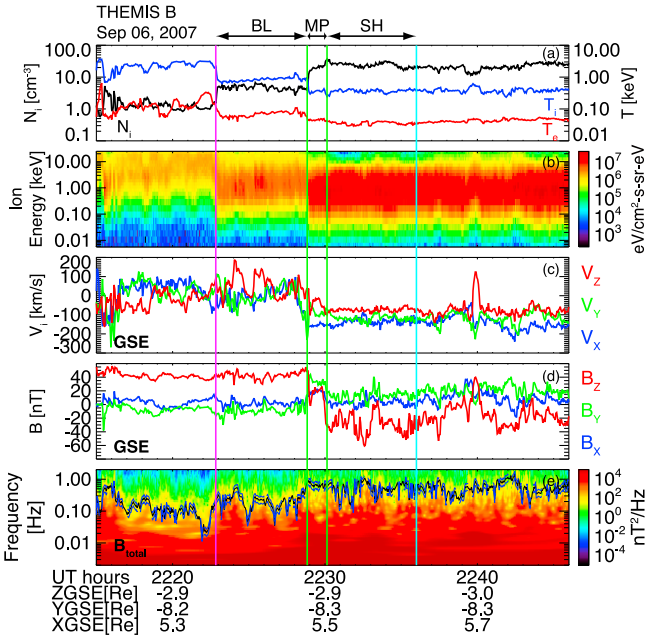

Figure 1. THEMIS B observations on September 6, 2007. (a) Ion density and average temperature of ions and elections referring to black, blue and red lines, respectively; (b) ion energy flux; (c) ion flow velocity in GSE coordinate; (d) magnetic field in GSE and (e) spectral energy density in B_{total}, black line corresponding to time series of frequency in spacecraft frame ($f_{s/c}$) at $f_{s/c} \approx v_{flow}/(2\pi\rho_i)$, two blue dashed lines corresponding to a $f_{s/c}$ range ±25% of $f_{s/c} \approx v_{flow}/(2\pi\rho_i)$. Four vertical lines from left to right referring to boundary layer inner edge (magenta), magnetopause inner edge (green), magnetopause outer edge (green) and edge (light blue) in magnetosheath (see text for details).

plasma and two plasma jets seen in positive V_Z flow velocities observed at 22:24 and 22:26 UT in the boundary layer shown in Figure 1c suggesting that the spacecraft is passing over the reconnection field lines with the X point located below the spacecraft. The boundary layer we identify in this case is therefore a consequence of the reconnection process and occurs largely on open field-lines. Figure 1e shows the wavelet spectrogram in total magnetic field (B_{total}). This reveals increasing spectral energy density at spacecraft frame frequencies below 1 *Hz* as the spacecraft transitions from the magnetosphere into the boundary layer and across the magnetopause where the largest amplitudes are found. It is these fluctuations, which form the subject of this paper.

[5] We have compiled a database of wave observations derived from 389 THEMIS magnetopause crossings similar to the case study example shown in Figure 1 for all B_{Z_sheath} orientations from years 2007–2009. In each case, the boundary layer (BL), magnetopause (MP) and magnetosheath (SH) intervals observed with each crossing have been identified from the summary plots similar to Figure 1 by visual inspection as described above. We note that since we include both northward and southward orientations of B_{Z_sheath} we use the term boundary layer here in the general sense as that region with plasma properties, such as ion density and electron density and temperature, intermediate between those of the SH and magnetosphere and distinct from the MP in the sense that there is no appreciable change in the magnetic field. Averages of wave and plasma properties are compiled through each regions. The averaging window in the case of the BL and MP is defined by their width, and in the case of the SH we average over an interval extending from just outside the MP to 10 ρ_i outwards along the magnetopause normal [*Russell and Elphic*, 1979]. 10 ρ_i is known as typical thickness of magnetopause. For the SH region, it is not necessary to have a whole SH spacial interval between the MP and bow shock. The SH width defined as 10 ρ_i is to provide several gyroradii wave scales outside the magnetopause sufficient to derive wave properties and thin enough to pertain only to those waves just outside of the MP. This spatial interval also defines the time-range over which the value of B_{sheath} is determined. Since this interval is typically much greater than the wave periods of interest, B_{sheath} provides a meaningful measurement of background magnetic field in the magnetosheath just outside the magnetopause.

[6] For each traversal we evaluate the wave power spectra in the transverse magnetic field ($B_\perp$). These have a highly repeatable scaling and vary as $\sim f_{s/c}^{-1.5} - f_{s/c}^{-1.7}$ and $\sim f_{s/c}^{-2.9}$ at low and high spacecraft frame frequencies ($f_{s/c}$), respectively. The average of these is plotted in Figure 2a. The location of the breakpoint in $f_{s/c}$ between these dependencies varies with the plasma flow speed (v_{flow}) over the spacecraft as $f_{s/c} \approx v_{flow}/(2i\rho_i)$, where ρ_i is the ion gyro-radius derived from the observed ion distribution. The robustness of both the scaling and location of the breakpoint in $f_{s/c}$ makes it possible to specify the energy content in the fields fluctuations over the range from $f_{s/c}$ = 0.01–2 *Hz* at the magnetopause from a single measurement of the spectral energy density at $f_{s/c} \approx v_{flow}/(2\pi\rho_i)$. To apply this in a statistical manner we take measurements of the spectral energy density in nT^2/Hz from each of our measured spectra averaged over a frequency range ±25% of $f_{s/c} \approx v_{flow}/(2\pi\rho_i)$. Our studies show that this range always includes the spectral breakpoint and is shown by the shaded regions in Figure 2 and on the spectra of the case study example in Figure 1e.

[7] The constancy in spectral form observed suggests that we may be always observing the same wave modes. To aid in identifying these we have also determined the spectra of the coincident electric fields and plot in Figure 2b the value of $E_\perp/B_\perp$ normalized by the local Alfvén speed (v_A). This ratio is approximately constant over $f_{s/c} < v_{flow}/(2\pi\rho_i)$ with a value slightly larger than the v_A and at higher frequencies the ratio increases nearly linearly with $f_{s/c}$. This variation is consistent with that expected for kinetic Alfvén waves (KAWs) if $f_{s/c} \sim v_{flow}/\lambda$ (or alternatively $\omega_{s/c} \sim k v_{flow}$), where $k = 2\pi/\lambda$ and λ is the wavelength. To demonstrate this the solid, dotted and dashed curves show the expected $E_\perp/B_\perp$ result in each region for a number of wavenormal angles (θ_k) based on the relationship $|\frac{E_\perp}{B_\perp}| = v_A^2 |\frac{k_\parallel}{\omega}|(1 + k_\perp^2\rho_i^2)(1 - \frac{\omega^2}{\omega_{ci}^2})$. Significantly, agreement at $f_{s/c} \geq v_{flow}/(2\pi\rho_i)$ requires θ_k approaching almost 90°. This is internally consistent with our assumption that $f_{s/c} \sim v_{flow}/\lambda$ or more formally that $\omega \ll \omega_{s/c}$ in the expression $\omega_{s/c} = 2\pi f_{s/c} = \omega + \mathbf{k} \cdot \mathbf{v}_{flow}$. To show this we plot in Figure 2c the wave frequency (f) of KAWs as function of $f_{s/c}$ using the expression $\omega = k_\parallel v_A \sqrt{1 + k_\perp^2(\rho_i^2 + \rho_s^2) - \frac{\omega^2}{\omega_{ci}^2}(1 + k_\perp^2\rho_i^2)}$ [*Stasiewicz et al.*, 2000] for a number of θ_k. For θ_k greater than 80°

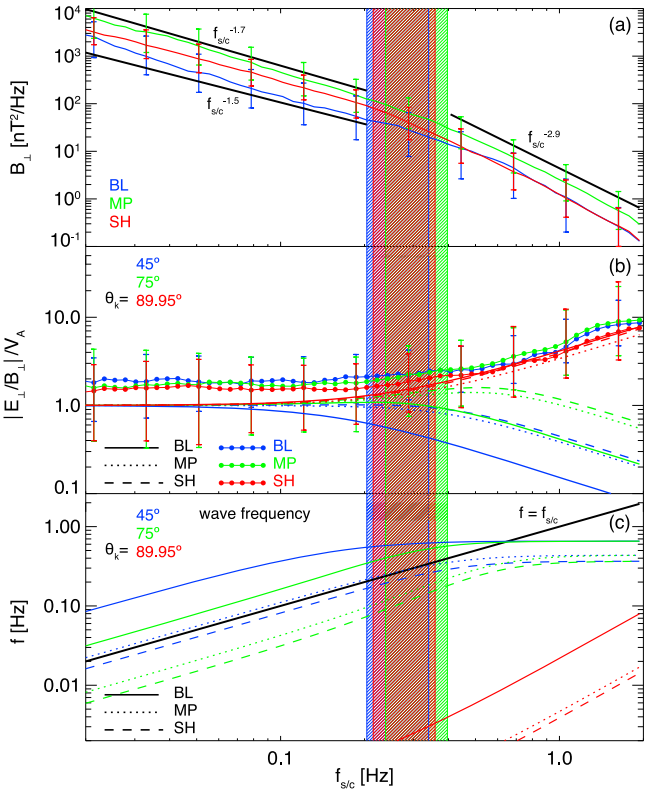

Figure 2. (a) Power spectral density of transverse magnetic field ($B_\perp$) as a function of frequency in spacecraft frame ($f_{s/c}$). Lines colored in blue, green and red corresponding to median wave spectrograms in different regions as boundary layer (BL), magnetopause layer (MP) and magnetosheath region (SH), respectively. Error bars determined by Boxplot, corresponding about 0.67 standard deviation around median value. (b) Comparison between observed $E_\perp/B_\perp$ (filled circle-lines blue, green, red referring to BL, MP, SH) ratio and theoretical predicted result (solid, dotted, dashed lines referring to BL, MP, SH) (both normalized by Alfvén speed) for all selected magnetopause crossing events in different regions and at different wavenormal angles (θ_k), 45°, 75°, 89.95° referring to blue, green and red, respectively. (c) Wave frequency (f) as a function of $f_{s/c}$ at different θ_k. At different θ_k, f in different regions is shown in different line styles. Black solid line corresponding to $f = f_{s/c}$.

we find that at $f_{s/c} = v_{flow}/(2\pi\rho_i)$ f for KAWs is less than $f_{s/c}$, and for those larger θ_k which provide the best fit to the observations shown in Figure 2b, f is an order or magnitude or more less than $f_{s/c}$. This result, the observed variation in $E_\perp/B_\perp$, and the location of the spectral breakpoint at $f_{s/c} \approx v_{flow}/(2\pi\rho_i)$ as expected from models of KAW turbulence [*Howes et al.*, 2008], provides a plausible case that for $f_{s/c} \geq v_{flow}/(2\pi\rho_i)$ we are observing Doppler shifted KAWs in the spacecraft frame. We note that this is consistent with a smaller study by *Chaston et al.* [2008], where interferometry was used to remove space-time ambiguity. Outside this range it is possible that the value of $E_\perp/B_\perp/v_A > 1$ found for $f_{s/c} < v_{flow}/(2\pi\rho_i)$ may be a consequence of non-local effects in shear Alfvén waves [*Chaston et al.*, 2007], where there may be large variations in the v_A over one parallel wavelength. Alternatively $E_\perp/B_\perp$ values larger than v_A over this range may be an indicator of the fast mode [*Johnson and Cheng*, 1997].

[8] Figure 3 shows distribution of spectral energy density ($\epsilon = (B_X^2 + B_Y^2 + B_Z^2)/\Delta f$ in nT^2/Hz) as a function of MLT under conditions of (a) positive (northward pointing) and (b) negative (southward pointing) B_{Z_sheath}. These results are equivalent to the distributions with northward and southward IMF respectively where the interplanetary magnetic field is usually propagated to the magnetopause from an upstream measurement [*Wing et al.*, 2005]. Moving outward from the center of the polar plots the three concentric circular grids correspond to the boundary layer (BL), magnetopause (MP) and magnetosheath (SH) regions, respectively. The color scale shows the logarithm of ϵ with black representing no data. The location of the magnetotail is represented by the black sector near midnight where for obvious reasons no MP traversals are recorded. In referring to these plots in the text the dawnside is taken to be from 4–12 MLT and the duskside from 12–20 MLT. These plots show that the largest ϵ irrespective of the orientation of B_{Z_sheath} is observed near noon and peaks in the SH just outside the MP with a distribution that favors the pre-noon hours.

[9] However at MLTs more than 2 hours either side of the noon we find ϵ peaks at the MP and is an order of magnitude larger on the dawn than duskside. Comparing Figures 3a and 3b shows that the distribution of ϵ in MLT is similar for both B_{Z_sheath} orientations. Exceptions include the 'hot spot' on the MP at 15 MLT for B_{Z_sheath} positive and the extension of large spectral energy densities to early morning hours on both the MP and BL for B_{Z_sheath} negative. Integrating over the entire spatial range surveyed shows that ϵ is larger for B_{Z_sheath} negative than B_{Z_sheath} positive.

[10] Figure 4 reveals the detailed dependence of these distributions with the degree of magnetic shear, $\theta_B = \cos^{-1}(\mathbf{B}_{sheath} \cdot \mathbf{B}_{sphere}/|\mathbf{B}_{sheath}||\mathbf{B}_{sphere}|)$, across the magnetopause. $\theta_B = 0°$ on the abcissae of these plots corresponds to aligned B_{sheath} and magnetospheric magnetic fields (B_{sphere}) fields whereas $\theta_B = 180°$ corresponds to anti-alignment. We note that while θ_B near 0° and 180° generally correspond to B_{Z_sheath} positive and negative respectively, for shear angle from 60°–120° this is not generally the case, since the B_{Z_sheath} does not show a clear relationship with θ_B, which means that B_{Z_sheath} can be positive or negative irrespective of whether $\theta_B < 90°$ or $\theta_B > 90°$ over this shear angle range after investigating their relationship in this study. From Figures 4a to 4c, relationships in dawn (3–10 MLT), noon (10–14 MLT) and dusk (14–21 MLT) sectors are shown. In each panel, blue, green and red square lines correspond to boundary layer (BL), magnetopause (MP), and magnetosheath region (SH), respectively. In general the spectral energy density (ϵ) in all three regions increase with θ_B. The most marked changes are however observed across the MP where we find nearly order of magnitude increases in ϵ on the dawn and dusk sectors for θ_B exceeding 60°. In the dawn sector ϵ at the MP also increases for the smallest θ_B.

3. Discussion and Conclusion

[11] These observations provide details of the global distribution and nature of electromagnetic field fluctuations

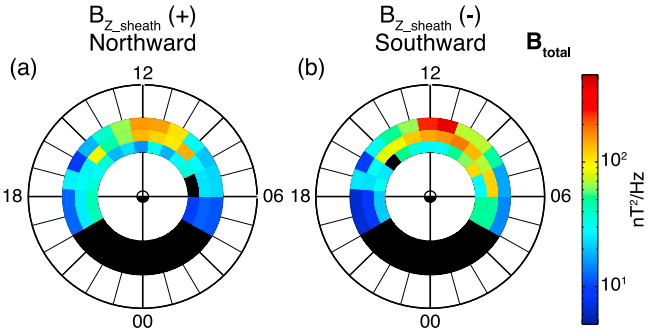

Figure 3. The polar map of power spectral density of total magnetic field as a function of magnetic local time (MLT) in XGSE-YGSE plane under conditions of (a) positive (northward pointing) and (b) negative (southward pointing) B_{Z_sheath}. Three concentric circular grids from inside to outside corresponding to boundary layer (BL), magnetopause layer (MP) and magnetosheath region (SH), as defined in the text, respectively.

across the Earth's magnetopause. The statistics we have provided pertain to observations at scales of a Doppler shifted ion gyro-radius, however we note that because of the robust power law scaling of spectral energy density (ϵ) with spacecraft frame frequency ($f_{s/c}$) observed, this measurement provides a proxy for the energy content in electromagnetic field fluctuations over the entire $f_{s/c}$ range sampled (0.01–2 *Hz*). We find for $f_{s/c} \geq v_{flow}/(2\pi\rho_i)$ that the dispersive properties of these fluctuations are consistent with that expected for kinetic Alfvén waves (KAWs) with phase speeds less than the flow speed. However we note that this does not necessarily eliminate the possibility of other modes being present. These waves are observed at all MLTs surveyed, but have largest amplitudes near noon, where they peak in the magnetosheath just outside the magnetopause. Away from noon however peak ϵ is observed on the magnetopause and an asymmetry in the distribution of ϵ is observed which favors the pre-noon/dawnside. This distribution can in part be qualitatively understood as a consequence of magnetosheath flow around the magnetopause, where these slowly propagating waves 'pile-up' in the depletion layer, just outside the magnetopause and progressively propagate inwards across field lines as they convect tailward with the flow. However this does not account for the dawn-dusk asymmetry through the magnetopause and boundary layer. This may be a consequence of location on the magnetopause downstream from a quasi-perpendicular vs quasi-parallel shock. It is known for instance that turbulence levels downstream from a quasi-parallel shock are significantly enhanced relative to that found downstream of a quasi-perpendicular shock [*Shevyrev and Zastenker*, 2005] and for a Parker spiral a quasi-parallel orientation is expected on the morning side. *Wing et al.* [2005] also suggested that the dawn-dusk asymmetry could be introduced by an asymmetry in the source of compressions, which could be driven directly in the solar wind.

[12] Importantly, we observe a magnetic shear (θ_B) dependence, which provides the largest spectral energy densities at the magnetopause under conditions of θ_B exceeding 60°. This may be consistent with either mode conversion from fast mode waves as previously reported by *Johnson et al.* [2001], which leads to a sharp increase in KAW power spectral density beyond around 50° θ_B and enhancement ϵ on the magnetopause for B_{Z_sheath} negative similar to observation, or reconnection which has been shown to drive broad spectrum of KAWs as described previously in a case study by *Chaston et al.* [2005]. Distinguishing mechanisms requires the association of enhanced spectral energy densities under conditions of large θ_B with reconnection outflow jets or the observation of KAWs radiating from the Alfvén resonance on the magnetopause. This study has not as yet been performed.

[13] Finally we note that since cross-field diffusion coefficients and the efficiency of scattering in gyro-radii scale field fluctuations (or KAWs) are proportional to spectral energy density (ϵ) [*Johnson and Cheng*, 1997], the distributions we have derived are proxies for the efficacy of the cross-field transport process. KAWs can heat ions perpendicular to the magnetic field line [*Johnson and Cheng*, 2001], consequently if KAWs are an important driver of cross-field transport, similar distributions in ϵ and heated transported magnetosheath ions should be observed. Previous studies have found that magnetosheath ions have higher temperatures and densities when observed in the dawnside magnetosphere than the duskside during northward IMF [*Hasegawa et al.*, 2003; *Wing et al.*, 2005]. This morphology may be associated with the gyro-scale magnetic field structure (or KAW) distributions shown in the Figure 3a for positive (northward) B_{Z_sheath} where an enhancement in ϵ is observed over the pre-noon hours on the magnetopause. Magnetosheath ions entering the magnetosphere at these

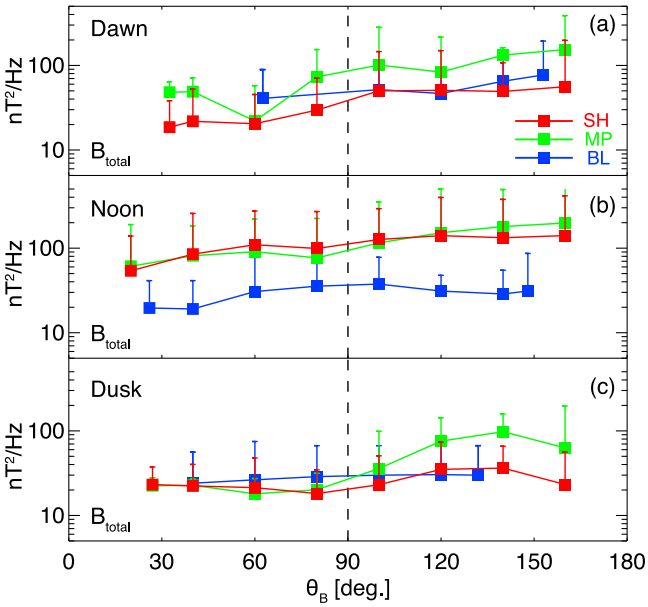

Figure 4. Variation of power spectral density of total magnetic field as a function of magnetic shear angle (θ_B). Different magnetic local time sectors, (a) dawn, (b) noon and (c) dusk. In each panel, blue, green and red lines corresponding to the relationship in boundary layer (BL), magnetopause layer (MP) and magnetosheath region (SH), respectively. Since logarithmic y-axis, error bars are plotted just in upper direction.

local times through the action of these gyro-scale structures could then continue to stream tailward in the flow through the boundary layer to account for the $-X_{GSE}$ extent of the enhanced dawnside magnetosheath fluxes in the magnetosphere. Under condition of negative B_{Z_sheath} to our knowledge there are no reported studies of the spatial distribution of magnetosheath plasmas in the magnetosphere with which to compare our results. It might be expected that magnetic reconnection dominates as a means for plasma entry into the magnetosphere under this condition, however we are unable to quantify the relative contributions from each process in this study. Nonetheless, the results for positive B_{Z_sheath} show that the dawn-dusk asymmetry observed in magnetosheath plasmas within the magnetosphere is qualitatively consistent with transport through the action of gyro-radii field structures (or KAWs) on plasmas across the magnetopause.

[14] **Acknowledgments.** This research was supported by NASA grant NNX09AF49G and NSF grants ATM-0612614 and ATM-0602728. THEMIS is made possible by NASA NAS5-02099, and the FGM team acknowledges support from DLR under contract 50 OC 030. The work by KHG was financially supported by the German Ministerium für Wirtschaft und Technologie and the Deutsches Zentrum für Luft- und Raumfahrt under grant 50QP0402. The authors also wish to thank J. P. McFadden for providing ESA data from THEMIS satellites.

[15] The Editor thanks two anonymous reviewers for their assistance in evaluating this paper.

References

Auster, H. U., et al. (2008), The THEMIS fluxgate magnetometer, *Space Sci. Rev.*, *141*, 235.

Chaston, C., et al. (2005), Drift-kinetic Alfvén waves observed near a reconnection X line in the Earth's magnetopause, *Phys. Rev. Lett.*, *95*, 065002.

Chaston, C., et al. (2007), Mode conversion and anomalous transport in Kelvin-Helmholtz vortices and kinetic Alfvén waves at the Earth's magnetopause, *Phys. Rev. Lett.*, *99*, 175004.

Chaston, C., et al. (2008), Turbulent heating and cross-field transport near the magnetopause from THEMIS, *Geophys. Res. Lett.*, *35*, L17S08, doi:10.1029/2008GL033601.

Hasegawa, A., and L. Chen (1975), Kinetic process of the plasma heating by Alfvén wave, *Phys. Rev. Lett.*, *35*, 370.

Hasegawa, A., and K. Mima (1978), Anomalous transport produced by kinetic Alfvén wave turbulence, *J. Geophys. Res.*, *83*, 1117.

Hasegawa, H., M. Fujimoto, K. Maezawa, Y. Saito, and T. Mukai (2003), Geotail observations of the dayside outer boundary region: Interplanetary magnetic field control and dawn-dusk asymmetry, *J. Geophys. Res.*, *108*(A4), 1163, doi:10.1029/2002JA009667.

Howes, G. G., S. C. Cowley, W. Dorland, G. W. Hammett, E. Quataert, and A. A. Schekochihin (2008), A model of turbulence in magnetized plasmas: Implications for the dissipation range in the solar wind, *J. Geophys. Res.*, *113*, A05103, doi:10.1029/2007JA012665.

Johnson, J. R., and C. Z. Cheng (1997), Kinetic Alfvén waves and plasma transport at the magnetopause, *Geophys. Res. Lett.*, *24*, 1423.

Johnson, J. R., and C. Z. Cheng (2001), Stochastic ion heating at the magnetopause due to kinetic Alfvén waves, *Geophys. Res. Lett.*, *28*, 4421.

Johnson, J. R., C. Z. Cheng, and P. Song (2001), Signatures of mode conversion and kinetic Alfvén waves at the magnetopause, *Geophys. Res. Lett.*, *28*, 227.

Lee, L. C., J. R. Johnson, and Z. W. Ma (1994), Kinetic Alfvén waves as a source of plasma transport at the dayside magnetopause, *J. Geophys. Res.*, *99*, 17,405.

McFadden, J. P., et al. (2008), The THEMIS ESA plasma instrument and in-flight calibration, *Space Sci. Rev.*, *141*, 277.

Mozer, F. S., et al. (2002), Evidence of diffusion regions at a subsolar magnetopause crossing, *Phys. Rev. Lett.*, *89*, 015002.

Nishino, M. N., et al. (2007), Geotail observations of temperature anisotropy of the two-component protons in the dusk plasma sheet, *Ann. Geophys.*, *25*, 769.

Paschmann, G. (1997), The magnetopause, *Space Sci. Rev.*, *80*, 217.

Rezeau, L., A. Morane, S. Perraut, A. Roux, and R. Schmidt (1989), Characterization of Alfvénic fluctuations in the magnetopause boundary layer, *J. Geophys. Res.*, *94*, 101.

Russell, C. T., and R. C. Elphic (1979), ISEE observations of flux transfer events at the dayside magnetopause, *Geophys. Res. Lett.*, *6*, 33.

Shevyrev, N. N., and G. N. Zastenker (2005), Some features of the plasma flow in the magnetosheath behind quasi-parallel and quasi-perpendicular bow shocks, *Planet. Space Sci.*, *53*, 95.

Sibeck, D. G., and V. Angelopoulos (2008), THEMIS science objectives and mission phases, *Space Sci. Rev.*, *141*, 35.

Stasiewicz, K., et al. (2000), Small scale Alfvénic structure in the aurora, *Space Sci. Rev.*, *92*, 423.

Wing, S., J. R. Johnson, P. T. Newell, and C.-I. Meng (2005), Dawn-dusk asymmetries, ion spectra, and sources in the northward interplanetary magnetic field plasma sheet, *J. Geophys. Res.*, *110*, A08205, doi:10.1029/2005JA011086.

V. Angelopoulos, Institute for Geophysical and Planetary Physics, University of California, Los Angeles, CA 90095-1567, USA (vassilis@ucla.edu)

C. C. Chaston and Y. Yao, Space Sciences Laboratory, University of California, Berkeley, CA 94720-7450, USA. (ccc@ssl.berkeley.edu; yyao@ssl.berkeley.edu)

K.-H. Glassmeier, Institut für Geophysik und Extraterrestrische Physik, Technische Universität Braunschweig, Mendelssohnstr. 3, D-38106 Braunschweig, Germany. (kh.glassmeier@tu-bs.de)